cmgh
CELLULAR AND MOLECULAR GASTROENTEROLOGY AND HEPATOLOGY

ORIGINAL RESEARCH

Hepatocyte FoxO1 Deficiency Protects From Liver Fibrosis via Reducing Inflammation and TGF-β1-mediated HSC Activation

Quan Pan,[1,*] Mingming Gao,[2,*] DaMi Kim,[1] Weiqi Ai,[1] Wanbao Yang,[1] Wen Jiang,[1] Wesley Brashear,[3] Yujiao Dai,[2] Sha Li,[2] Yuxiang Sun,[1] Yajuan Qi,[2] and Shaodong Guo[1]

[1]Department of Nutrition, College of Agriculture and Life Sciences, Texas A&M University, College Station, Texas; [2]Department of Pharmacology, School of Basic Medical Science, North China University of Science and Technology. Tangshan, China; and [3]High Performance Research Computing, Texas A&M University, College Station, Texas

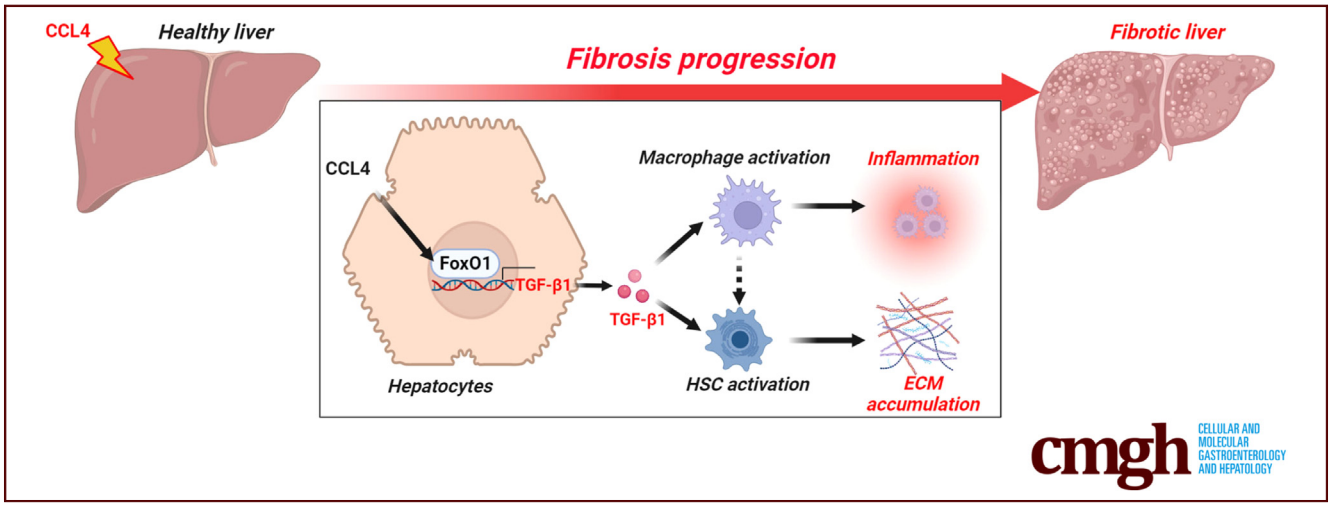

SUMMARY

Hepatocytes Foxo1 controls the crosstalk between hepatocytes, macrophages, and hepatic stellate cells, via regulating TGF-β1 expression, to promote liver fibrosis. Hepatic FoxO1 may be a therapeutic target for prevention and treatment of liver fibrosis.

BACKGROUND & AIMS: The O-class of the forkhead transcription factor FoxO1 is a crucial factor mediating insulin→PI3K→Akt signaling and governs diverse cellular processes. However, the role of hepatocyte FoxO1 in liver fibrosis has not been well-established. In his study, we investigated the role of hepatocyte FoxO1 in liver fibrosis and uncovered the underlying mechanisms.

METHODS: Liver fibrosis was established by carbon tetrachloride (CCL4) administration and compared between liver-specific deletion of FoxO1 deletion (F1KO) and control (CNTR) mice. Using genetic and bioinformatic strategies in vitro and in vivo, the role of hepatic FoxO1 in liver fibrosis and associated mechanisms was established.

RESULTS: Increased FoxO1 expression and FoxO1 signaling activation were observed in CCL4-induced fibrosis. Hepatic FoxO1 deletion largely attenuated CCL4-induced liver injury and fibrosis compared with CNTR mice. F1KO mice showed ameliorated CCL4-induced hepatic inflammation and decreased TGF-β1 mRNA and protein levels compared with those of CNTR mice. In primary hepatocytes, FoxO1 deficiency reduced TGF-β1 expression and secretion. Conditioned medium (CM) collected from wild-type hepatocytes treated with CCL4 activated human HSC cell line (LX-2); such effect was attenuated by FoxO1 deletion in primary hepatocytes or neutralization of TGF-β1 in the CM using TGF-β1 antibody. Hepatic FoxO1 overexpression in CNTR mice promoted CCL4-induced HSC activation; such effect was blocked in L-TGF-β1KO mice.

CONCLUSIONS: Hepatic FoxO1 mediates CCL4-inducled liver fibrosis via upregulating hepatocyte TGF-β1 expression, stimulating hepatic inflammation and TGF-β1-mediated HSC activation. Hepatic FoxO1 may be a therapeutic target for prevention and treatment of liver fibrosis. *(Cell Mol Gastroenterol Hepatol 2024;17:41–58; https://doi.org/10.1016/j.jcmgh.2023.08.013)*

Keywords: FoxO1; Hepatic Stellate Cell; Inflammation; Liver Fibrosis; TGF-β1.

Liver fibrosis, resulting from chronic liver damage with excessive accumulation of extracellular matrix proteins, is a common cause of liver failure and morbidity and causes serious health burden worldwide.[1] Several causes could lead to the development of liver fibrosis, including alcohol consumption, nonalcoholic steatohepatitis (NASH), viral hepatitis, autoimmune hepatitis, nonalcoholic fatty liver disease (NAFLD), and cholestatic liver diseases.[2] An increasing number of novel targets and signaling pathways including apoptosis, oxidative stress, inflammation, epigenetics and receptor-mediated signals have been identified to be involved in the process of liver fibrosis.[3] However, the pathogenesis of chronic liver injury and fibrosis has not been fully elucidated.[4]

TGF-β1, belonging to the TGF-β superfamily, is the most potent mediator for fibrogenesis.[5–7] TGF-β1 plays a pivotal role in a diverse range of cellular responses, including cell proliferation, apoptosis, differentiation, migration, adhesion, angiogenesis, and extracellular matrix (ECM) synthesis.[8] After secretion from hepatocytes and Kupffer cells and activation following hepatotoxicant injury or other pathology, TGF-β1 is activated and binds to the type II (TβRII) receptor, interacting with and phosphorylating the type I receptor (TβRI). This results in recruitment and phosphorylation of intracellular Smad2 and Smad3, which interact with Smad4 to form a transcriptionally active complex that enhances TGF-β1-responsive gene expression, including alpha-smooth muscle actin (αSMA) and collagens. This stimulates the translation of hepatic stellate cells (HSCs) to a myofibroblast-like phenotype and inhibits ECM degradation through increasing expression of tissue inhibitor of matrix metalloproteinases (TIMPs).[5,9] Importantly, overexpression of TGF-β1 in hepatocytes promotes liver fibrosis and failure.[7,10,11] Treatment of hepatocytes with TGF-β1 increases fibrogenesis and apoptosis, in a Smad3-dependent manner, which is antagonized by Smad7.[12–14]

The O-class of the forkhead transcription factor FoxO1 is a crucial factor mediating the action of insulin → PI3K → Akt and regulates cell growth, metabolism, and survival.[15,16] Foxo1 promotes gluconeogenic, autophagic, pro-apoptotic, and pro-inflammatory gene expression, which are suppressed via FoxO1-S253 phosphorylation downstream of PI3K and Akt by insulin[17–24] and estrogen.[25] Through binding to the conserved insulin response element-CAAAACAA on the promoter of target genes, Foxo1 stimulates expression of G6pc (gluconeogenesis), Tat (tyrosine catabolism), LC3 (autophagy induction), Bim (apoptosis), angiotensinogen (hypertension), heme-oxygenase-1, and Tlr4 (inflammation),[20,23,24,26,27] governing diverse cellular processes. Diminished insulin action by deleting the hepatic insulin receptor or both IRS1 and IRS2 genes in mice results in liver failure[28,29]; this is largely due to FoxO1 activation, which causes mitochondria dysfunction.[30] Moreover, Akt-mediated FoxO1 inhibition has been shown to be required for liver regeneration after partial hysterectomy.[31] However, how hepatocyte FoxO1 contributes to the pathogenesis of liver fibrosis has not been fully investigated. In this study, we evaluated FoxO1 expression and FoxO1 signaling activation in carbon tetrachloride (CCL4)-induced mouse liver fibrosis model. Using our liver specific FoxO1 knock out mice (F1KO), we investigated the role of hepatocyte FoxO1 in control of liver fibrosis and explored the underlying mechanisms. We found that hepatic FoxO1 mediates CCL4-inducled liver fibrosis via stimulating hepatic inflammation and TGF-β1-mediated HSC activation, which suggests that a crosstalk exists between hepatocytes and HSC via FoxO1-regualted TGF-β1. Thus, hepatocyte FoxO1 is a potential therapeutic target for prevention and treatment of liver fibrosis.

Results

FoxO1 is Upregulated in CCL_4-induced Liver Fibrosis in Mice

To induce liver fibrosis in mice, we injected 20% solution of CCL4 intraperitoneally (ip) twice per week for 4 weeks (2.5 ul/g body weight) in wild-type (WT) mice. Compared with the oil group, the CCL4 group showed significantly lower body weight and liver weight, but higher liver weight to body weight ratio (Figure 1*A*–*C*). CCL4 administration dramatically elevated serum alanine transaminase (ALT) and aspartate transaminase (AST) levels (Figure 1*D* and *E*) and caused severe liver fibrosis and increased HSC activation, represented by Sirius red staining and αSMA staining, respectively (Figure 1*F*). These observations demonstrate that this CCL4 administration model is highly effective in inducing liver injury and fibrosis in mice. We next determined the FoxO1 expression in the liver of these mice and found that FoxO1 protein levels were significantly increased in the CCL4-induced fibrotic liver, especially in the cytoplasm and nucleus of hepatocytes (Figure 1*F*). The activation of FoxO1 was further confirmed in primary hepatocytes with increased nuclear FoxO1 upon CCL4 treatment (Figure 1*G*). These results suggest the potential involvement of hepatocyte FoxO1 in control of liver injury and fibrosis. RNA sequencing (RNAseq) analysis on the liver of CCL4- or oil-treated mice demonstrated that hepatic expression of hundreds of genes were altered by

***Authors share co-first authorship.**

Abbreviations used in this paper: **ALT, alanine transaminase; ALP, alkaline phosphatase; αSMA, alpha-smooth muscle actin; AST, aspartate transaminase; CCL, carbon tetrachloride; CM, conditioned medium; CNTR, control; DEGs, differently expressed genes; DMEM, Dulbecco's Modified Eagle Medium; ECM, extracellular matrix; F1KO, FoxO1 deletion; FBS, fetal bovine serum; H&E, hematoxylin and eosin; HSC, hepatic stellate cell; ip, intraperitoneally; KEGG, Kyoto Encyclopedia of Genes and Genomes; MDA, malonaldehyde; NAFLD, nonalcoholic fatty liver disease; NASH, nonalcoholic steatohepatitis; NPCs, non-parenchymal cells; P/S, penicillin-streptomycin; PBMCs, peripheral blood mononuclear cells; PBS, phosphate-buffered saline; qPCR, quantitative polymerase chain reaction; RNAseq, RNA sequencing; SOD, superoxide dismutase; TIMP, tissue inhibitor of matrix metalloproteinase; WT, wild-type.**

Most current article

2352-345X
https://doi.org/10.1016/j.jcmgh.2023.08.013

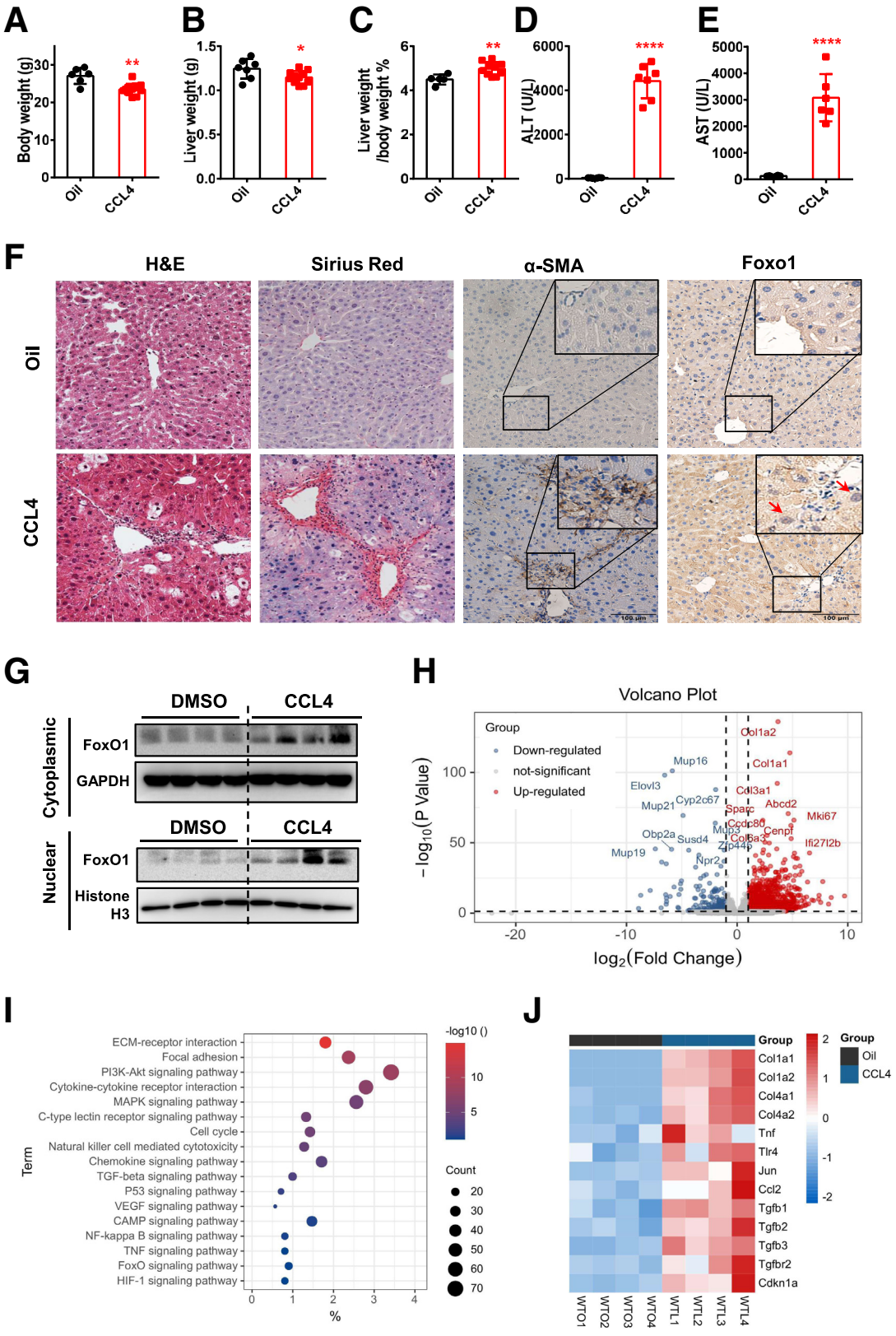

Figure 1. FoxO1 is upregulated in CCl_4-induced liver fibrosis in mice. WT male mice at 8- to 10-weeks of age were administrated with corn oil or 20% solution of CCL4 (2.5 ul/g body weight, ip, twice/week) for 4 weeks (n = 7). Serum ALT, AST, body weight (*A*), liver weight (*B*), liver weight to body weight ratio (*C*), serum ALT levels (*D*), and serum AST levels (*E*) of oil- and CCL4-treated mice. (*F*) H&E, Sirius red staining, and immunohistochemistry for FoxO1 and αSMA of the liver section of oil- and CCL4-treated mice. (*G*) Cytoplasmic and nuclear FoxO1 protein levels in primary hepatocytes treated with CCL4 (n = 4). (*H*) Volcano plot of DEGs in the liver of oil- or CCL4-treated WT mice (n = 4). (*I*) KEGG analysis of upregulated genes in the liver of CCL4-treated compared with oil-treated mice (n = 4). (*J*) Heatmap of selected DEGs related to liver fibrosis, inflammation, and TGF-β1 signaling (n = 4). Data are presented as the means ± standard error of the means. *$P < .05$; **$P < .01$; ****$P < .0001$ vs oil using Student *t*-test.

CCL4 administration (Figure 1*H*). Further Kyoto Encyclopedia of Genes and Genomes (KEGG) pathway analysis indicated that genes involved in ECM-receptor interaction and TGF-β signaling pathways (fibrosis), NF-kappa-β signaling and TNF signaling pathways (inflammation) are upregulated (Figure 1*I* and *J*). Moreover, hepatic FoxO1 signaling pathway was also activated by CCL4 administration (Figure 1*I*). These results suggest a potential role of hepatocyte FoxO1 in control of CCL4-induced liver fibrosis in mice.

Hepatic FoxO1 Deficiency Protects From CCL4-induced Liver Injury and Fibrosis in Mice

To investigate the role of hepatocyte FoxO1 in control of liver injury and fibrosis, we generated liver-specific F1KO mice and injected F1KO and control (CNTR, Foxo1 L/L) mice with CCL4 for 4 weeks. Contrary to CNTR mice, CCL4-induced alterations in body weight, liver weight, and liver weight to body weight ratio were not observed in F1KO mice (Figure 2*A*). Under CCL4 administration, although FoxO1 deficiency did not affect CCL4-induced alterations of serum alkaline phosphatase (ALP), albumin, total bilirubin, direct bilirubin, and total bile acid levels, F1KO mice showed significantly lower serum AST, ALT, and total protein levels compared with those of CNTR mice (Figure 3*A*), suggesting a protective effect of hepatic FoxO1 deficiency on CCL4-induced liver injury. Moreover, we found that CCL4-treated F1KO mice exhibited significantly higher superoxide dismutase (SOD) levels but lower malonaldehyde (MDA) levels in the liver compared with those of CCL4-treated CNTR mice, suggesting a protective role of hepatic FoxO1 deficiency on CCL4-induced oxidative stress in the liver (Figure 2*B*).

Next, we determined the effects of hepatic FoxO1 deficiency on the development of liver fibrosis and found that CCL4-treated F1KO mice showed less fibrotic area and HSC activation compared with CCL4-treated CNTR mice (Figure 3*B*). CCL4 stimulated increase of hepatic *Col1* and *Acta2* (encoding αSMA protein) mRNA and protein levels was attenuated in F1KO mice compared with CNTR mice (Figure 3*C* and *D*). Similarly, CCL4-promoted Mmp2, Mmp9, Mmp12, and TIMP1 mRNA expression were also significantly lower in the liver of F1KO mice compared with those of CNTR mice (Figures 3*C* and 2*C*). These results suggest that hepatic FoxO1 deletion protects mice from CCL4-induced liver fibrosis.

Hepatic FoxO1 Deficiency Ameliorates CCL4-induced Liver Inflammation

RNAseq analysis on the liver of CCL4-treated CNTR and F1KO mice showed that hundreds of genes were differentially expressed between CNTR and F1KO liver (Figure 4*A*). More than 90% of these differently expressed genes (DEGs) were downregulated in F1KO mouse liver, indicating that hepatocytes FoxO1 activation is required for the expression of these genes during CCL4-induced liver fibrosis (Figure 4*A*). We further performed KEGG pathway analysis on these downregulated genes and found that these FoxO1 regulated genes are mainly involved in inflammatory response pathways, such as NF-kappa B, Toll-like receptor, and TNF signaling pathways, which were shown to be activated upon CCL4 administration (Figures 1*I* and 4*B*). These results suggest that FoxO1 could be a key mediator of CCL4-induced liver inflammation, which was further confirmed by quantitative polymerase chain reaction (qPCR) analysis of hepatic inflammatory response markers expression. CCL4-stimulated *Tnfa* (by 54-fold), *Il1b* (by 8-fold), *Il11*(by 4.5-fold), *and iNos* (by 2.2-fold) mRNA expressions were largely diminished by hepatic FoxO1 deletion ($P < .01$) (Figure 4*C*).

During liver injury, abundant circulating monocytes and macrophages are recruited to the injured liver tissue and are involved in the augmentation liver inflammation and liver fibrosis.[32,33] We next collected peripheral blood mononuclear cells (PBMCs) from CCL4-treated CNTR and F1KO mice and performed flow cytometric analysis (Figure 5*A* and *B*). Ly6C^{hi} monocytes are inflammatory monocyte subset. Ly6C^{hi}CCR2^{+} subset shows higher migratory and infiltration capacity and are preferentially recruited into inflamed tissue.[34] Although the ratio of Ly6C^{hi} monocytes in the PBMCs of CCL4-treated CNTR and F1KO mice were comparable, F1KO mice showed significantly lower amount of Ly6C^{hig}CCR2^{+} monocytes in PBMCs, and more than 20% decrease of CCR2 intensity in Ly6C^{hig}CCR2^{+} monocytes, suggesting that hepatic FoxO1 deletion decreased recruitment of inflammatory monocytes and macrophages to injured liver upon CCL4 administration ($P < .05$) (Figure 4*D*–*F*). Hepatic monocytes, especially macrophages, are central in the pathogenesis of liver injury and fibrosis.[35] We next collected non-parenchymal cells (NPCs) from the liver of CCL4-treated CNTR and F1KO mice and observed a 17% decrease of TNFα expression in neutrophils and a 46% decrease of IL-1β in macrophages in the F1KO mouse liver compared with those of CNTR mice, indicating a protective role in CCL4-induced liver inflammation by hepatic FoxO1 deletion ($P < .05$) (Figures 4*G*, *H* and 5*C*, *D*).

CCL4 Stimulates Hepatocyte TGF-β1 Expression and Secretion via FoxO1

TGF-β1 is a master of liver fibrosis. TGF-β1 signaling activates HSCs and increases the ECM, and further promotes liver fibrosis progression.[36] In addition to downregulating inflammatory response-related genes, hepatic FoxO1 deletion also attenuated hepatic TGF-β signaling pathway upon CCL4 administration (Figure 4*B*). Several hepatic TGF-β signaling pathway-related genes, including TGF-β1, TGF-β3, Tgfbr1, and Tgfbr2, were dramatically decreased in the liver of CCL4-treated F1KO mice compared with those of CNTR mice (Figure 6*A*). The downregulation of TGF-β1 by hepatic FoxO1 deletion was further confirmed by qPCR and Western blot analysis with significantly decreased hepatic TGF-β1 mRNA (by 52%) and protein (49%) levels in F1KO mice ($P < .05$) (Figure 6*B* and *C*). Further immunohistochemical staining of TGF-β1 in the liver confirmed that CCL4 increased TGF-β1 levels in the liver of CNTR mice, especially

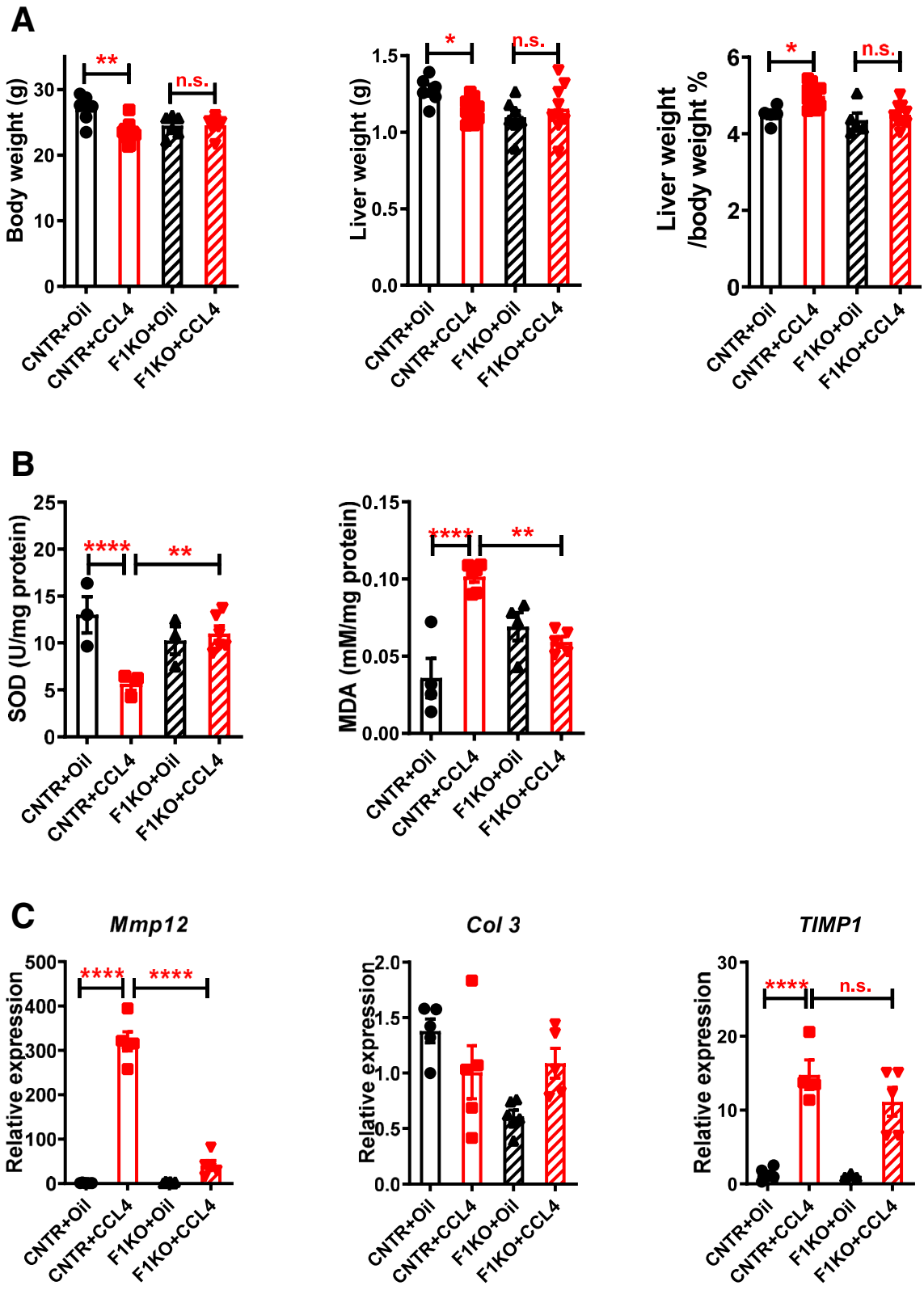

Figure 2. Characteristics of WT and Liver-specific Foxo1 knockout (F1KO) mice with CCL4 injection. Liver F1KO male mice and their littermates (CNTR, FoxO1 L/L) at 8- to 10-weeks of age were administrated with corn oil or 20% solution of CCL4 (2.5 ul/g body weight, ip, twice/week) for 4 weeks. (*A*) Body weight, liver weight, and liver to body weight ratio of these mice (n = 7). (*B*) SOD and MDA levels in the liver of these mice (n = 3-5). (*C*) mRNA levels of *Col 3, Mmp12*, and *TIMP1* in the liver of these mice (n = 4-5). Data are presented as the means ± standard error of the means. *$P < .05$; **$P < .01$; ****$P < .0001$ vs oil using Student *t*-test.

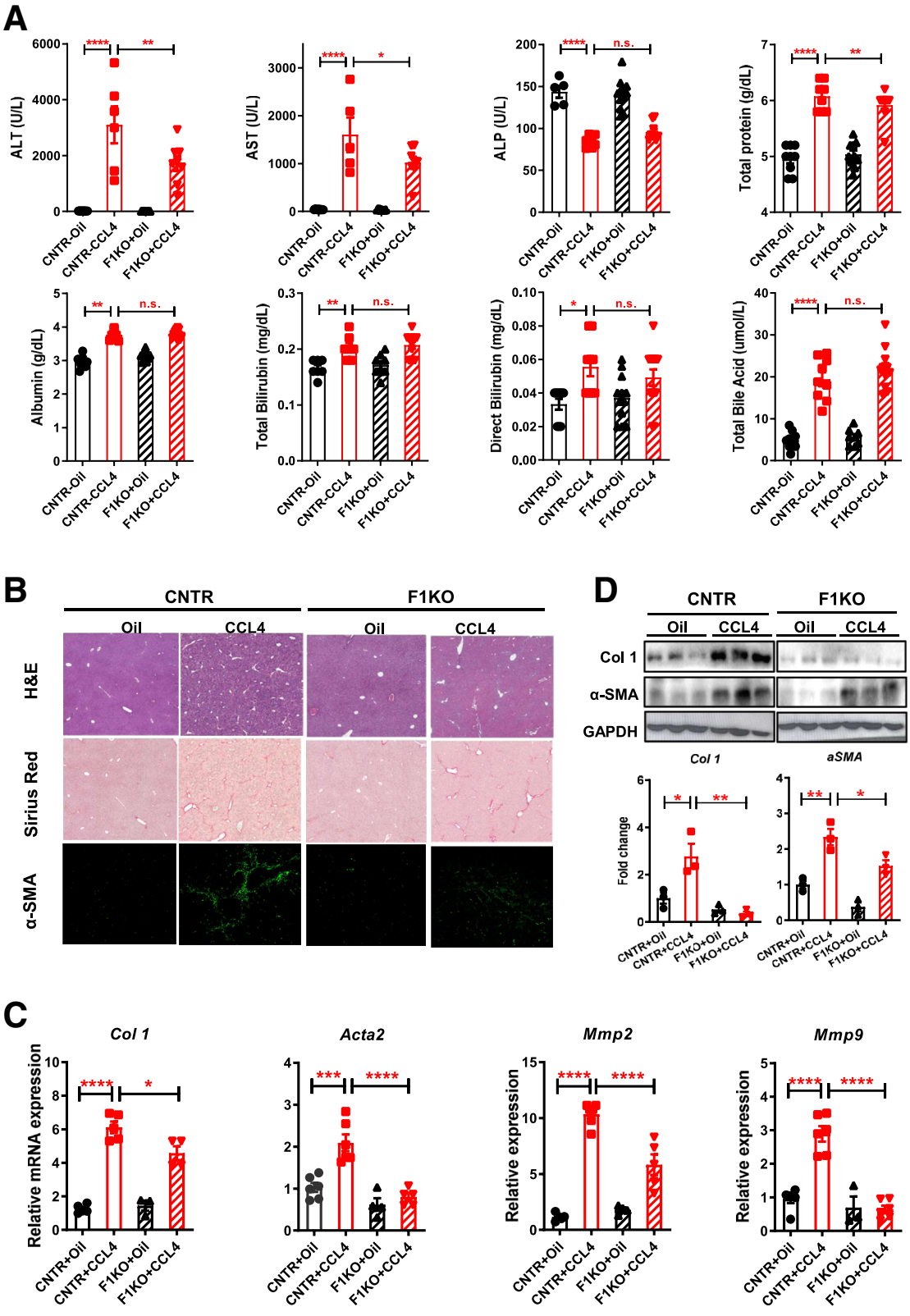

Figure 3. Hepatic FoxO1 deficiency protects from CCL4-induced liver injury and fibrosis in mice. Liver F1KO male mice and their littermates (CNTR, FoxO1 L/L) at 8- to 10-weeks of age were administrated with corn oil or 20% solution of CCL4 (2.5 ul/g body weight, ip, twice/week) for 4 weeks. (*A*) Serum ALT, AST, ALP, total protein, albumin, total bilirubin, direct bilirubin, and total bile acid levels of these mice (n = 6-13). (*B*) H&E, Sirius red staining and IF staining for αSMA of the liver section of these mice (n = 3). (*C*) mRNA levels of *Col1, Acta2, Mmp2*, and *Mmp9* in the liver of these mice (n = 4-7). (*D*) Western blot analysis and corresponding quantification of Col1, αSMA, and GAPDH protein levels in the liver of these mice (n = 3). Data are presented as the means ± standard error of the means. *$P < .05$; **$P < .01$; ****$P < .0001$ between assigned groups using 1-way analysis of variance.

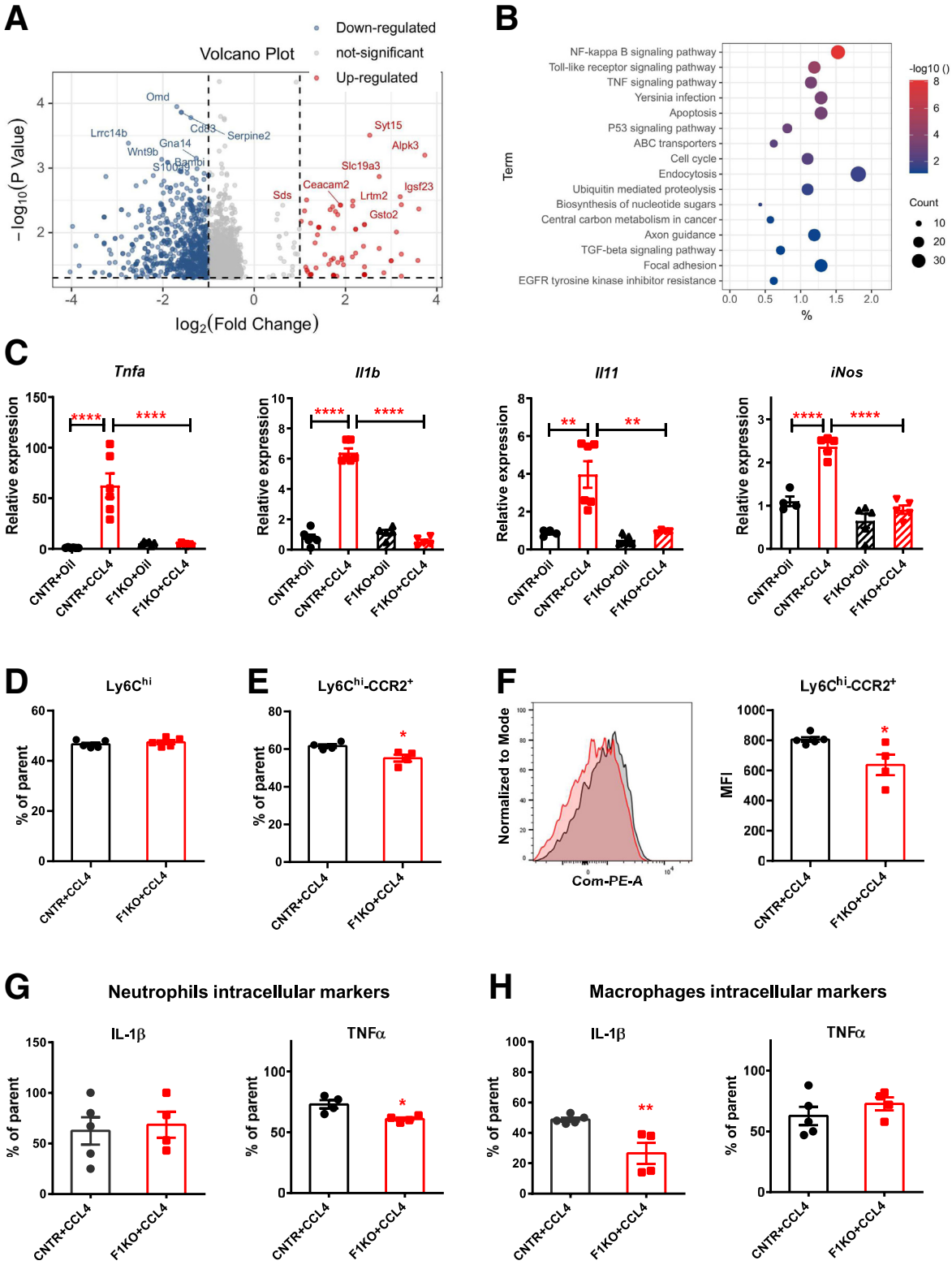

Figure 4. Hepatic FoxO1 deficiency ameliorates CCL4-induced liver inflammation. (*A*) Volcano plot of DEGs in the liver of CNTR and F1KO mice (n = 4). (*B*) KEGG analysis of downregulated genes in the liver of CCL4-treated F1KO mice compared with CCL4-treated CNTR mice (n = 4). (*C*) mRNA levels of *Tnfα, Il1b, Il-11*, and *iNos* in the liver of these mice (n = 4-6). (*D–F*) PBMCs of CCL4 treated CNTR and F1KO mice were collected, percentage of Ly6C^{hi} monocytes (*D*) and Ly6C^{hi}-CCR2^{+} monocytes (*E*), and mean fluorescence intensity (MFI) of CCR2 in Ly6C^{hi}-CCR2^{+} monocytes were determined by flow cytometry analysis (n = 4-5). (*G* and *H*) Liver NPCs of CCL4-treated CNTR and F1KO mice were collected for flow cytometry analysis. Intracellular TNFα and IL-1β levels in neutrophils (*G*) and macrophages (*H*) were determined by flow cytometry analysis (n = 4-5). Data are presented as the means ± standard error of the means. *$P < .05$; **$P < .01$; ****$P < .0001$ between assigned groups using 1-way analysis of variance or between CNTR + CCL4 and F1KO + CCL4 groups using Student *t*-test.

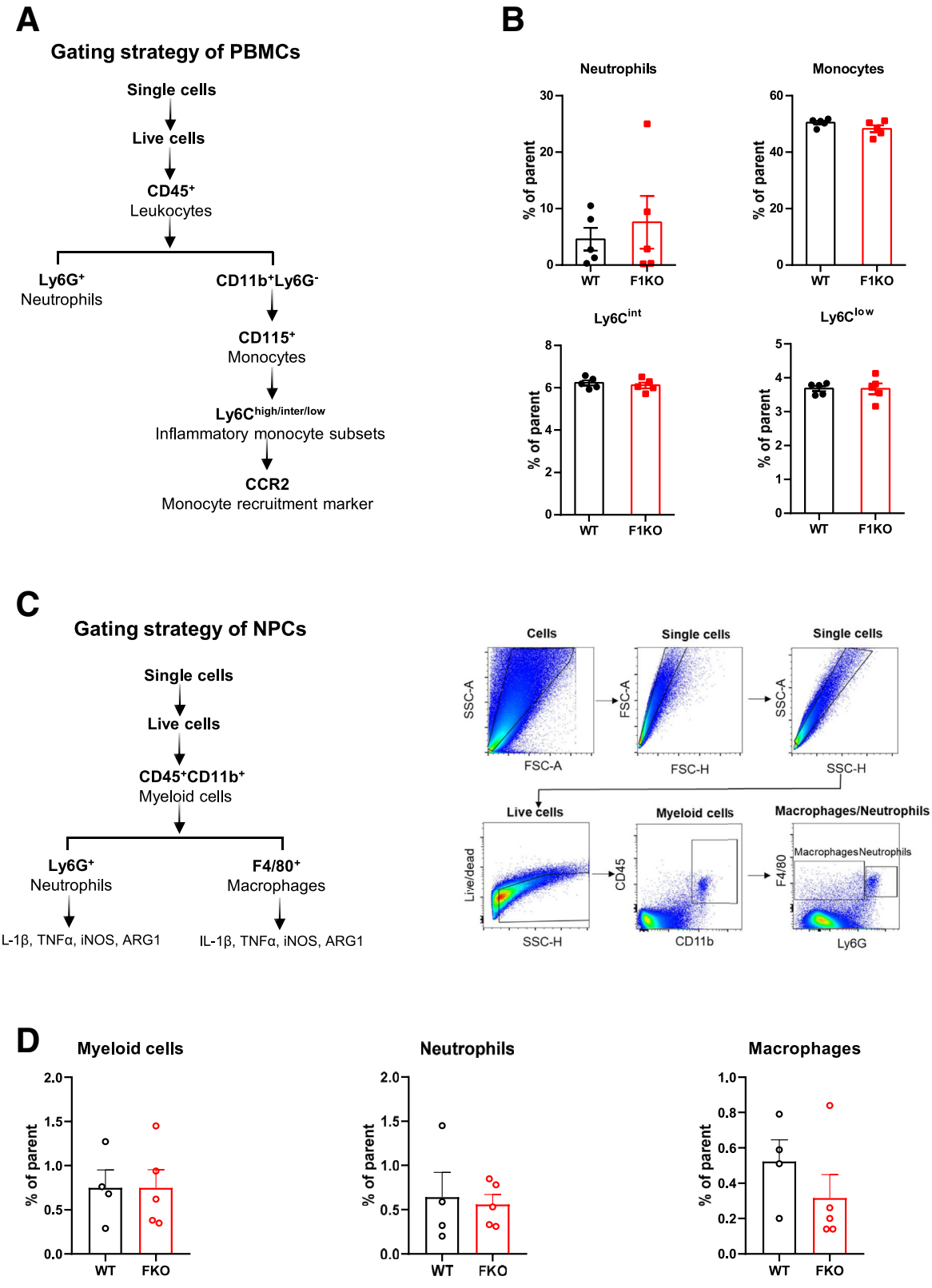

Figure 5. Flow gating strategy and inflammatory profile characterization in PBMCs and NPCs of WT and F1KO mice. (*A*) Flow cytometry gating strategy of PBMCs. (*B*) Percentage of neutrophils, monocytes, Ly6C^{int} and Ly6C^{low} subsets in PBMCs of WT and F1KO mice (n = 5). (*C*) Flow cytometry gating strategy and representative scatter-blots of flow cytometry analysis of NPCs. (*D*) Percentage of total myeloid cells, neutrophil, and macrophage subsets in liver NPC of WT and F1KO mice (n = 4-5). Data are presented as the means ± standard error of the means.

in the hepatocytes; such effect was largely attenuated in F1KO mice (Figure 6*D*). Furthermore, we isolated primary hepatocytes from CNTR and F1KO mice with acute CCL4 administration and detected TGF-β1 secretion from these cells. We found that FoxO1 deletion dramatically decreased TGF-β1 secretion from hepatocytes isolated from CCL4 treated mice by 79% ($P < .0001$) (Figure 6*E*). These results suggest that hepatocyte FoxO1 is a key regulator of CCL4-induced TGF-β1 expression and secretion in the liver, specifically in hepatocytes.

To further confirm the regulation of TGF-β1 expression and secretion by FoxO1 in hepatocytes, we performed in vitro studies with primary hepatocytes isolated from CNTR and F1KO mice. CCL4-treated CNTR hepatocytes showed increased TGF-β1 mRNA and protein levels, as well as FoxO1 levels (Figure 6*F* and *G*), which is consistent with the elevated FoxO1 levels observed in the liver of CCL4-treated CNTR mice (Figure 1*F* and *G*). However, CCL4-treated F1KO hepatocytes exhibited significantly lower TGF-β1 mRNA and protein levels compared with those of CCL4 treated CNTR cells (Figure 6*F* and *G*). CCL4-stimulated TGF-β1 secretion from primary hepatocytes was also reduced by 28% by FoxO1 deletion ($P < .01$) (Figure 6*H*). Taken together, CCL4 stimulates hepatocyte TGF-β1 expression and secretion via FoxO1.

Hepatocyte FoxO1 → TGF-β1 Axis Promotes HSC Activation

HSC activation and ECM production are central in the pathogenesis of liver fibrosis.[36] Given that hepatic FoxO1 deletion attenuated CCL4-induced HSCs activation and ECM production in vivo (Figure 3*B–D*), we next tested whether the FoxO1 in hepatocytes could directly impact HSC activation in vitro. We treated human HSC cell line LX-2 with conditioned medium (CM) collected from CCL4-treated CNTR and F1KO primary hepatocytes and found that CM from both CCL4-treated CNTR and F1KO hepatocytes dramatically promoted αSMA protein levels in LX-2 cells, indicating the activation of HSCs (Figure 7*A*). Interestingly, LX-2 cells treated with CM from F1KO hepatocytes showed less αSMA protein levels compared with cells treated with CM from CNTR hepatocytes (Figure 7*A*). These results suggest a paracrine activation of HSCs controlled by hepatocyte FoxO1.

In the current study, we have reported that FoxO1 controlled the CCL4-stimulated hepatocyte TGF-β1 expression and secretion (Figure 6); we next tested whether the FoxO1-regulated crosstalk between hepatocytes and HSCs was mediated by TGF-β1. We used TGF-β1 antibody (α-TGF-β1) to neutralize TGF-β1 in CM from hepatocytes and determined the effect of TGF-β1 neutralization on HSC activation. Compared with CM from CNTR hepatocytes without CCL4 treatment, CM from CCL4-treated CNTR hepatocytes are more effective to activate TGF-β1 signaling, represented by pSmad3 levels, to promote LX-2 activation (Figure 7*B*). TGF-β1 neutralization of CM from CCL4-treated CNTR hepatocytes attenuated the TGF-β1 signaling activation and LX-2 cells activation, suggesting that hepatocyte secreted TGF-β1 is a mediator of the crosstalk between hepatocytes and HSCs and promotes HSC activation in response to CCL4 administration (Figure 7*B*). FoxO1 deletion in hepatocytes ameliorated such crosstalk, and TGF-β1 neutralization of CM from F1KO hepatocytes further attenuated HSCs activation (Figure 7*B*). These observations demonstrate that hepatocytes FoxO1 → TGF-β1 axis controls a crosstalk between hepatocytes and HSCs to promote HSC activation in response to CCL4 administration in vitro.

To further validate this concept in vivo, we generated hepatocyte-specific TGF-β1 deletion (L-TGF-β1KO) mice and overexpressed FoxO1 by adenovirus (ad-FoxO1) (tail vein injection) in L-TGF-β1KO mice and control (CNTR, TGF-β1 L/L) mice. We then subjected these mice to acute CCL4 administration and determined the TGF-β1 signaling and HSC activation. In TGF-β1 L/L mice, FoxO1 overexpression promoted the mRNA and protein levels of *Tgfb1* and *αSMA* in the liver, as well as TGF-β1 signaling activation (Figure 7*C* and *E*), indicating that FoxO1 promotes TGF-β1 expression and HSC activation in response to CCL4 administration in vivo. However, in L-TGF-β1KO mice, no significant differences of hepatic *Tgfb1* and *αSMA* levels and TGF-β1 signaling activation were observed between ad-GFP and ad-FoxO1 groups (Figure 7*D* and *F*). These results suggest that hepatic FoxO1 promoted HSC activation in vivo upon CCL4 administration is hepatocyte TGF-β1-dependent. Interestingly, we also found that FoxO1 overexpression increased mRNA expression of inflammatory genes *Tnfα* (by 1.8-fold) and *Mcp1* (by 4.5-fold) in the liver of TGF-β1 L/L mice, whereas such effects were diminished in L-TGF-β1KO mice, demonstrating that hepatic FoxO1 → TGF-β1 axis also controls the inflammatory response in the liver upon CCL4 stimulation ($P < .05$) (Figure 7*C* and *D*).

Hepatic TGF-β1 Deficiency Ameliorates CCL4-induced Liver Fibrosis

We further validated the role of hepatocyte TGF-β1 in CCL4-induced liver fibrosis. Under CCL4 administration, although hepatic TGF-β1 deficiency did not affect CCL4-induced alterations of serum ALP, total bilirubin, direct bilirubin, and total bile acid levels, L-TGF-β1KO mice showed significantly lower serum AST, ALT, total protein, and albumin levels compared with those of CNTR mice (Figure 8*A*), suggesting a protective effect of hepatocyte TGF-β1 deficiency on CCL4-induced liver injury. Hematoxylin and eosin (H&E) and Sirius red staining results showed that hepatic TGF-β1 deficiency markedly ameliorated CCL4-induced liver damage and fibrosis (Figure 8*B*). Although oil-treated L-TGF-β1KO mice showed similar hepatic hepatocyte TGF-β1 mRNA levels as oil-treated CNTR mice, hepatic TGF-β1 deficiency almost blocked CCL4 stimulated increase of *Tgfb1* mRNA levels (Figure 8*C*), suggesting that hepatocyte TGF-β1 is a major contributor or at least a key initiator of CCL4-stimulated TGF-β1 expression in the liver. Moreover, hepatic TGF-β1 deficiency attenuated CCL4-induced increase of *Acta2* and *Col1* mRNA levels (Figure 8*C*),

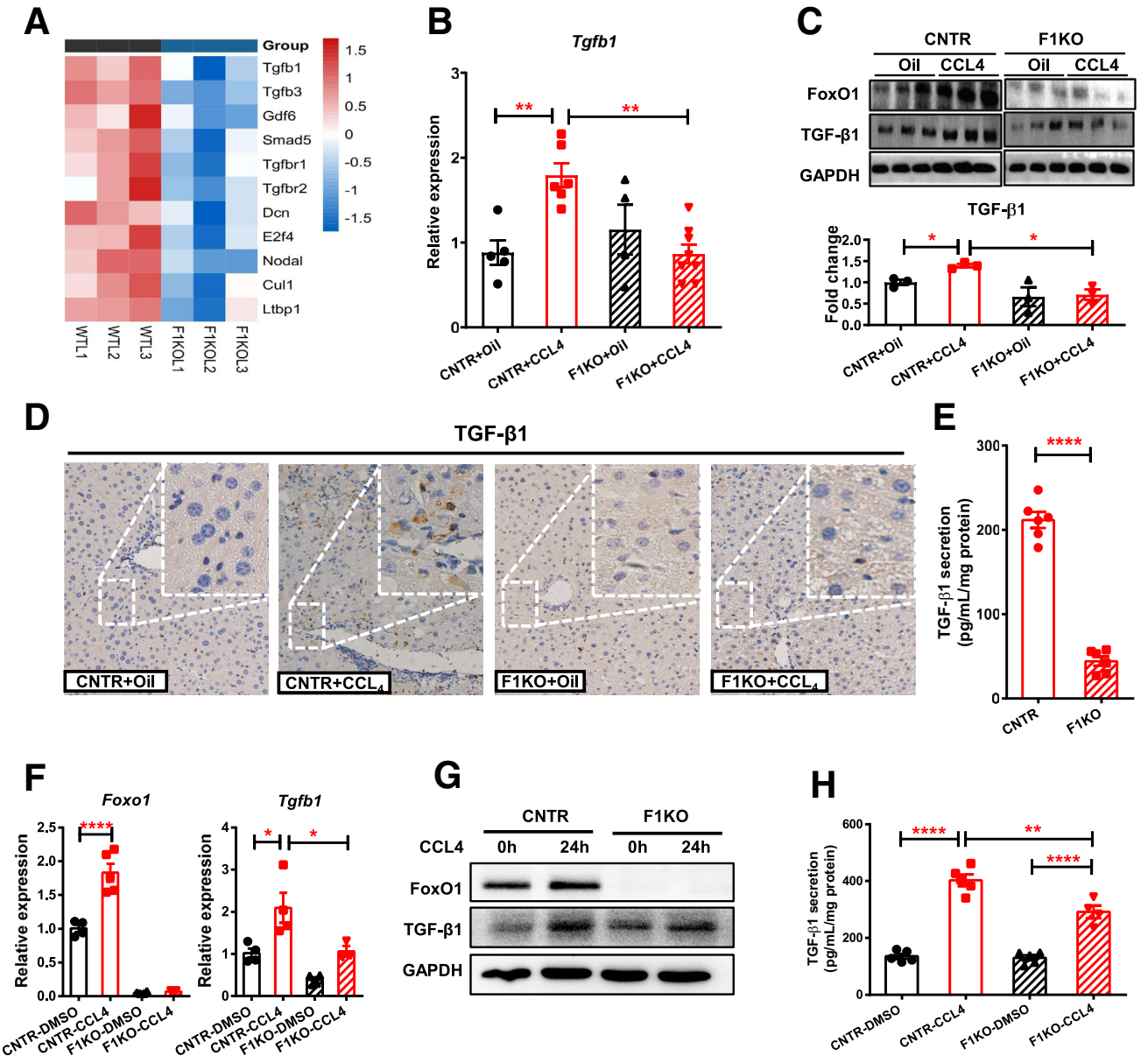

Figure 6. CCL4 stimulates hepatocyte TGF-β1 expression and secretion via FoxO1. (*A–C*) CNTR and F1KO male mice at 8- to 10-weeks of age were administrated with corn oil or 20% solution of CCL4 (2.5 ul/g body weight, ip, twice/week) for 4 weeks. (*A*) Heatmap of selected DEGs related to TGF-β signaling (n = 3). (*B*) TGF-β1 mRNA levels in the liver of oil- and CCL4-treated mice (n = 4-7); (*C*) Western blot analysis and quantification of TGF-β1 protein levels in the liver of oil- and CCL4-treated mice (n = 3); (*D*) Immunohistochemisty staining for TGF-β1 of the liver section of oil- and CCL4-treated mice (n = 3). (*E*) CNTR and F1KO male mice at 8- to 10-weeks of age were administrated with one dose of 20% solution of CCL4 (2.5 ul/g body weight, ip). Primary hepatocytes were isolated from CNTR and F1KO mice 20 hours after CCL4 administration and cultured in serum-free DMEM medium for 24 hours; the media were collected to determine TGF-β1 levels by ELISA kit (n = 6). (*F*) Primary hepatocytes were isolated from CNTR and F1KO mice, then subjected to 2.5 mM CCL4 treatment for 12 hours. *Foxo1* and *Tgfb1* mRNA levels in these cells were determined by qPCR (n = 4). (*G* and *H*) Primary hepatocytes were isolated from CNTR and F1KO mice, then subjected to 2.5 mM CCL4 treatment for 24 hours. (*G*) FoxO1 and TGF-β1 protein levels in these cells were determined by Western blot analysis (N = 3). (*H*) Cell culture media were collected to determine TGF-β1 levels by ELISA kit (n = 4-5). Data are presented as the means ± standard error of the means. *$P < .05$; **$P < .01$; ***$P < .001$; ****$P < .0001$ between assigned groups using 1-way analysis of variance.

indicating a key role of hepatocyte TGF-β1 in control of HSC activation and ECM production in CCL4-induced liver fibrosis. Western blot analysis of the liver of oil- and CCL4-treated CNTR and L-TGF-β1KO mice demonstrated that hepatocyte TGF-β1 is required for CCL4-stimulated TGF-β1 signaling activation and HSC activation in the liver (Figure 8*D*). Taken together, our results support the idea that hepatocyte TGF-β1 plays a key role in HSC activation,

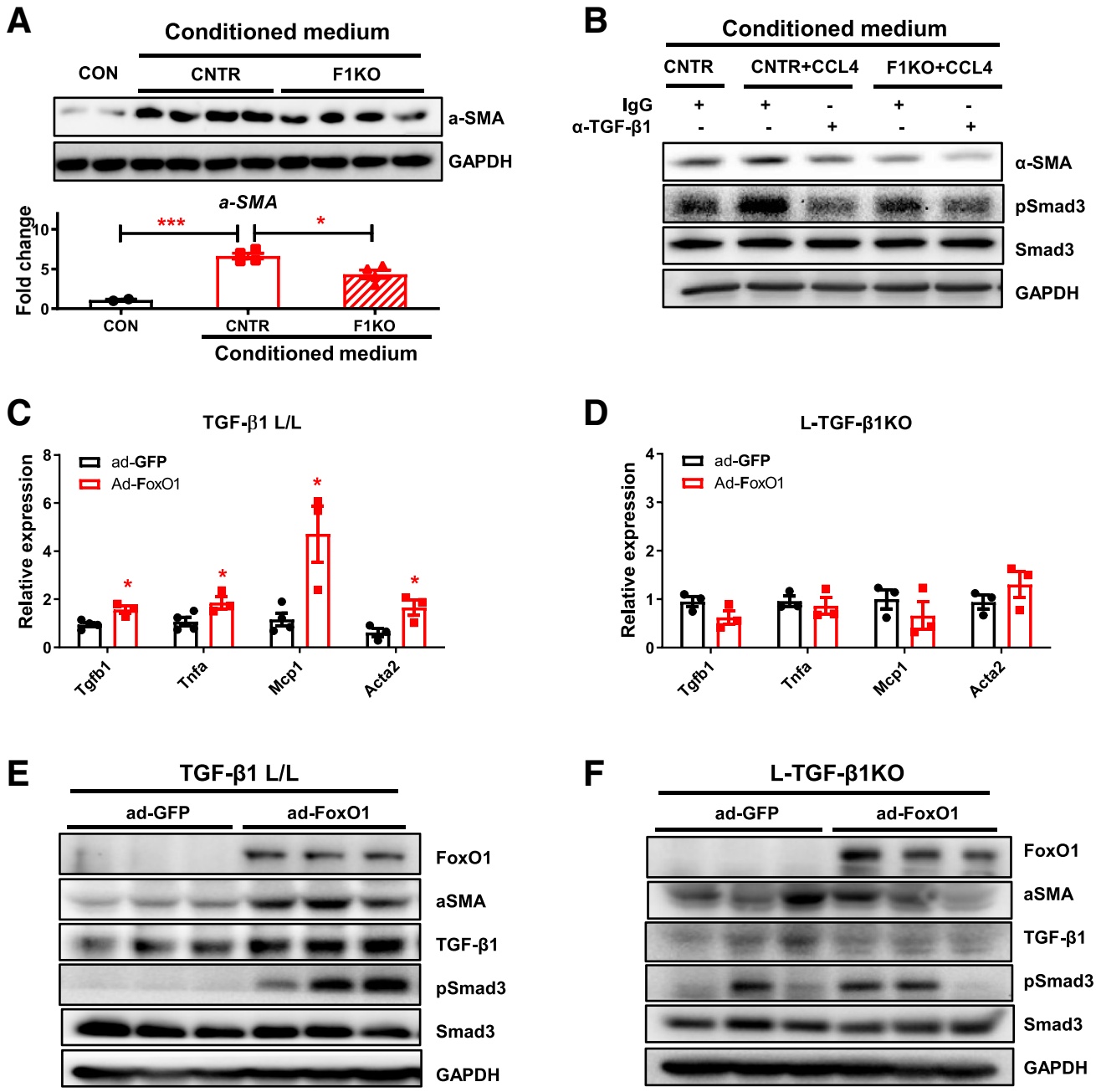

Figure 7. Hepatocytes FoxO1→TGF-β1 axis promotes HSC activation. (*A*) Primary hepatocytes were isolated from CNTR and F1KO mice, then subjected to 2.5 mM CCL4 treatment for 6 hours, then rinsed with PBS twice, and then cultured in serum-free DMEM medium for 24 hours. CM from these cells were collected to treat LX-2 cells for 12 hours. αSMA and GAPDH protein levels in LX-2 cells were determined by Western blot analysis (N = 3). (*B*) Primary hepatocytes were isolated from CNTR and F1KO mice, then subjected to 2.5 mM CCL4 treatment for 6 hours, then rinsed with PBS twice, and then cultured in serum-free DMEM medium for 18 hours. CM from these cells were collected and then subjected to TGF-β1 neutralization with TGF-β1 antibody (0.5 μg/mL), normal mouse IgG1 used as control. The neutralized CM was used to treat LX-2 cells for 12 hours. αSMA, pSmad3, Smad3 and GAPDH protein levels in LX-2 cells were determined by Western blot analysis (N = 3). (*C–F*) L-TGF-β1KO and TGF-β1 L/L male mice at 8- to 10-weeks of age were delivered with ad-GFP or ad-FoxO1 (1 X 10^9 pfu/mice, intravenous injection). Seven days after adenovirus delivery, mice were administrated with 1 dose of 20% solution of CCL4 (2.5 ul/g body weight, ip,). Liver tissues were harvested 20 hours after CCL4 administration. mRNA expression of *Tgfb1*, *Tnf*α, *Mcp1*, and *Acta2* in the liver of TGF-β1 L/L mice (*C*) and L-TGF-β1KO mice (*D*) were determined by qPCR. FoxO1, αSMA, TGF-β1, pSmad3, Smad3, and GAPDH protein levels in the liver of TGF-β1 L/L mice (*E*) and L-TGF-β1KO mice (*F*) were determined by Western blot analysis (n = 3). Data are presented as the means ± standard error of the means. *$P < .05$; ***$P < .001$ among assigned groups using 1-way analysis of variance or vs ad-GFP using Student *t*-test.

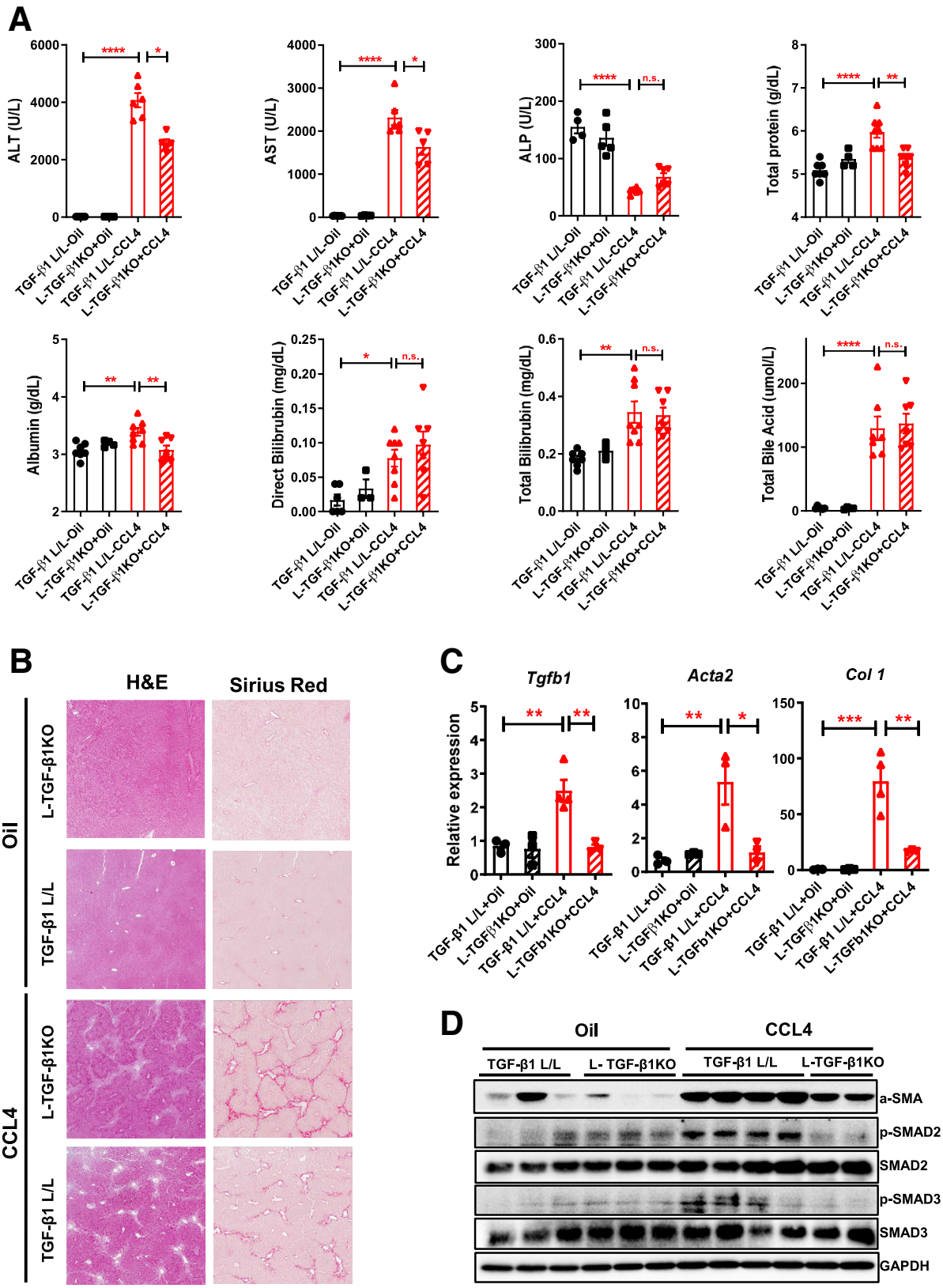

Figure 8. Hepatic TGF-β1 deficiency ameliorates CCL4-induced liver fibrosis. CNTR and L-TGF-β1KO male mice at 8- to 10-weeks of age were administrated with corn oil or 20% solution of CCL4 (2.5 ul/g body weight, ip, twice/week) for 4 weeks. (*A*) Serum ALT, AST, ALP, total protein, albumin, total bilirubin, direct bilirubin, and total bile acid levels of these mice (n = 4-8). (*B*) H&E and Sirius red staining of the liver section of these mice (n = 3). (*C*) Tgfb1, Acta2, and Col 1 mRNA levels in the liver of these mice (n = 3-4). (*D*) Western blot analysis of αSMA, pSmad2, Smad2, pSmad3, Smad3, and GAPDH protein levels in the livers of these mice (n = 2-4). Data are presented as the means ± standard error of the means. *$P < .05$; **$P < .01$; ***$P < .001$ between assigned groups using 1-way analysis of variance.

which in turn causes liver fibrosis in response to CCL4 treatment. Together with previous observations that hepatic FoxO1 deficiency protects mice from CCL4-induced liver injury and fibrosis (Figures 2, 3, and 4) and that hepatocytes FoxO1 → TGF-β1 axis promotes HSCs activation both in vitro and in vivo (Figure 6 and 7), our study may provide a novel therapeutic strategy via targeting hepatocyte FoxO1 → TGF-β1 axis to combat liver injury and fibrosis.

Discussion

In this study, we first provide genetic and bioinformatic evidence, establishing that hepatocyte FoxO1 is a key mediator of CCL4-induced liver injury and fibrosis. Our results present 4 important findings: (1) CCL4 administration elevates FoxO1 expression and promotes FoxO1 signaling activation in the liver of WT mouse; (2) hepatic FoxO1 deficiency ameliorates CCL4-induced liver injury and fibrosis; (3) hepatic FoxO1 deficiency attenuates CCL4-stimulated hepatic inflammation; and (4) hepatocytes FoxO1 → TGF-β1 axis promotes HSCs activation and mediates CCL4-indcued liver fibrosis. These findings suggest that hepatocyte FoxO1 could serve as a potential therapeutic target for the treatment of liver fibrosis.

The regulation of FoxO1 expression occurs at both transcriptional and post-transcriptional levels. In this study, we observed that CCL4 treatment promoted both FoxO1 mRNA and protein expression in hepatocytes, suggesting that CCL4-stimulated FoxO1 expression in the liver occurs, at least partially, at transcriptional levels. Previously, Sebastian and colleagues have shown that CCL4 challenge in mice promotes hepatic expression of E2F1, a transcription factor that regulates FoxO1 mRNA expression.[37,38] E2F1 is the potential mediator of CCL4-stimulated FoxO1 mRNA expression. Additionally, ROS also promotes the transcription of FoxO1.[39] In our study, we determined the oxidative stress in the liver of CCL4-treated mice and found that CCL4 reduced SOD and increased MDA levels, suggesting an elevation of oxidative stress by CCL4. CCL4 could increase FoxO1 mRNA expression via promoting ROS levels in the hepatocytes. Along with the transcriptional regulation of FoxO1, we also observed that CCL4 activated cAMP signaling pathway, which has been shown to promote FoxO1 stability via PKA mediated FoxO1 phosphorylation at ser S273 (FoxO1-S273).[40] Of note, hepatic PI3K-AKT signaling pathway, which stimulates FoxO1 degradation via FoxO1-S253 phosphorylation, was also activated by CCL4. One explanation to this paradox is that cAMP activation overrides the effect of PI3K-AKT signaling in control of FoxO1 protein level, as we have shown that constitutive phosphorylation at FoxO1-S273 blocks the insulin-PI3K-AKT signaling induced FoxO1 degradation.[40] These results suggest that FoxO1-S273 phosphorylation may be the key for the post-transcriptional regulation of FoxO1 by CCL4. Taken together, the regulation of FoxO1 expression by CCL4 occurs at both transcriptional and post-transcriptional levels.

The involvements of FoxO family in tissue fibrosis have been broadly investigated. However, the roles of FoxO1 in control of liver fibrosis are controversial. The study by Adachi and colleagues revealed that inhibition of FoxO1 in HSC by insulin-PI3K-AKT signaling promotes HSC activation and exacerbates bile duct ligation-induced liver fibrosis, concluding that FoxO1 is a suppressor of liver fibrosis.[41] In a diet-induced NAFLD mouse model, Pan and colleagues found that hepatic FoxO1/3/4 deletion accelerates the pathogenesis of liver fibrosis, suggesting that FoxO transcription factors protect against diet-induced NAFLD and liver fibrosis.[42] Contradictorily, Ding and colleagues found that FoxO1 inhibition protects HFD-induced NAFLD via attenuating ER stress and necroptosis, and Lee and colleagues demonstrated that myeloid FoxO1 deletion attenuated diet induced NASH and fibrosis.[43,44] Moreover, the study by Das and colleagues demonstrated that FoxO1 inactivation ameliorated iron-overload-induced liver fibrosis.[45] The discrepancies observed in these studies are mainly due to 2 aspects: (1) different liver fibrosis models were used in these studies. The underlying mechanisms of liver fibrosis largely vary in different models, given that FoxO1 governs diverse of cellular processes, it is possible that FoxO1 activation could have opposite effects on the pathogenesis of liver fibrosis in different models; (2) Different specificities of FoxO1 inhibition or deletion. In Adachi's study, globally heterozygous FoxO1 was deleted; the detrimental effects of FoxO1 deletion observed in their studies could be a consequence of FoxO1 deletion in cells other than HSCs. In Ding's and Das's studies, resveratrol or FoxO1 inhibitor were used to broadly block FoxO1 activity; the beneficial effects of FoxO1 inhibition were not specifically identified. Nevertheless, in our current study, with our hepatocyte FoxO1-specific knockout mice, we provided clear evidence that hepatocyte FoxO1 mediates CCL4-induced liver fibrosis in mice.

We uncovered that hepatocyte FoxO1 stimulates liver inflammation and TGF-β1-mediated HSC activation, and subsequently promotes CCL4-induced liver fibrosis. Hepatic macrophages are central in control of liver inflammation and the pathogenesis of liver fibrosis.[35] Our current study suggests that hepatocyte TGF-β1 is required for FoxO1-stimulated liver inflammation in CCL4-induced liver injury and fibrosis (Figure 7*C* and *D*). However, TGF-β1 treatment did not stimulate macrophages inflammatory response (data not shown). Apoptotic hepatocyte is a major trigger of macrophage activation following liver injury and plays key roles in control of liver fibrosis and injury.[46–49] Our previous studies demonstrated that hepatocyte-expressed TGF-β1 exerts autocrine effect to activate FoxO1 in hepatocytes and promotes hepatocyte apoptosis in a FoxO1-dependent manner.[50,51] Hepatocytes FoxO1 activation-induced macrophage inflammatory response is potentially mediated by TGF-β1 → FoxO1 signaling controlled hepatocytes apoptosis. Indeed, we observed reduced expression of genes involved in apoptosis in the liver of F1KO mice upon CCL4 administration (Figure 4*B*). Furthermore, we demonstrated that hepatocyte is a crucial source or at least a key initiator of CCL4-induced hepatic TGF-β1 expression (Figure 8*C*), which activates HSCs and promotes liver fibrosis upon CCL4 administration in mice. Hepatocyte TGF-β1 expression and secretion were promoted by CCL4 in a FoxO1-dependent

manner (Figure 6). Of note, macrophage is another major source of hepatic TGF-β1; it is possible that FoxO1 deficiency attenuates macrophage activation and reduces TGF-β1 expression in macrophage, which in turn attenuates the crosstalk between macrophages and HSCs in CCL4-treated mice. Nevertheless, our in vivo and in vitro results revealed a novel crosstalk between hepatocyte and HSCs that is controlled by hepatocytes FoxO1$\rightarrow$TGF-β1 axis. Supportively, Xu and colleagues also observed a TGF-β1-mediated crosstalk between hepatocyte and HSCs in promoting CCL4-induced liver fibrosis.[52] Such crosstalk has also been shown to contribute to hepatocellular carcinoma development.[53–55] These findings highlight the crucial role of hepatocyte TGF-β1 in the development of liver diseases. Previously, FoxO1 protein expression and nuclear localization in hepatocytes were shown to be elevated in patients with NASH compared with those of healthy controls.[56] Whether the concept that hepatocyte FoxO1$\rightarrow$TGF-β1 axis-controlled liver inflammation and HSC activation could apply to NASH development is unclear. Further studies with NASH models in F1KO mice are needed to validate the roles of hepatocyte FoxO1 in NASH development.

To be noted, compared with control mice, F1KO mice showed 45% and 36% decreases of ALT and AST, respectively, whereas L-TGF-β1KO mice had 36% and 26% decreases of ALT and AST, respectively (Figures 3*A* and 8*A*). These results suggest that mechanisms other than regulating TGF-β1 may be involved in the protective effect of FoxO1 deficiency on CCL4-induced liver injury and fibrosis. For example, inhibition of FoxO1 is required for liver regeneration.[31] Hepatic FoxO1 deficiency may protect CCL4-induced fibrosis via promoting liver regeneration. Moreover, in our current study, we found that FoxO1 deficiency attenuated CCL4-stimulated oxidative stress (Figure 2*B*), which potentially contributes to the decrease inflammation and fibrosis in the liver.[57] Moreover, FoxO1 promotes hepatocyte IL-6 expression, which has also been shown to mediate the crosstalk between hepatocytes and HSCs in CCL4-induced liver fibrosis.[58,59] Further studies with F1KO mice are needed to uncover other mediators between hepatocytes and NPCs and discover potential therapeutic targets for the prevention and treatment of liver injury and fibrosis.

Methods

Animal

The floxed Foxo1 (FoxO1 L/L) mice were generated as previously described.[40,60,61] The floxed TGF-β1 mice (TGF-β1L/L) and Albumin-Cre mice were purchased from Jackson Lab. To generate liver-specific FoxO1 or TGF-β1 knockout mice, FoxO1 L/L mice or TGF-β1L/L mice were crossed with Albumin-Cre mice, respectively. The tail DNA of pups was genotyped by PCR and then confirmed by DNA sequencing analysis. All mice used in this study were male and maintained at 22 °C in a 12/12 hour light-dark cycle and given free access to food and water. If not specified elsewhere, all the mice were male at 8- to 12-weeks of age. All animal experiments were performed according to procedures approved by Texas A&M University Institutional Animal Care and Use Committee, and all animals were randomly assigned to cohorts when used.

CCL4 Injection

For acute CCL4 administration, mice were challenged with 1 dose of corn oil or 20% solution of CCL4 (2.5 ul/g body weight, ip injection), and then euthanized for tissue harvest 20 hours after CCL4 injection. For chronic CCL4 administration, mice were challenged with corn oil or 20% solution of CCL4 (2.5 ul/g body weight, ip, twice/week) for 4 weeks, and then euthanized for tissue harvest 72 hours after CCL4 injection.

Detection of Antioxidant Indexes

We removed the liver tissue from the −80 °C refrigerator and placed it in a 5-ml EP tube. We added the per-chilled homogenization medium or saline according to the volume of homogenization medium or saline volume: liver volume = 9:1 This was ground in an ice water bath and centrifuge (centrifugal conditions: 4 °C, 3000 r/min, 10 minutes), and we drew the supernatant fluid to obtain liver protein homogenization. Then we added physiological saline to dilute it 100 times, added the sample according to the sample addition table, and used the micro plate reader to detect the absorbance of the sample and calculated the concentration of the sample to be measured.

Detection of SOD Protein Expression in the Liver of Mice

The liver protein homogenization was prepared in the same way, and the protein expression of MDA in the liver of mice.

Quantitative Real-time PCR

Total RNA was extracted from tissue or cells with TRIzol reagent (Invitrogen) and reversely transcribed to cDNA with the iScript cDNA synthesis system (Bio-Rad) according to manufacturer's instructions. Quantitative gene expression was measured using gene-specific primers (Table 1) using the SYBER Green Supermix system (Bio-Rad), as previously described.[51] The expression of cyclophilin served as the internal control. Gene expression was analyzed with standard ΔΔCt method of real-time PCR, and results were presented as relative fold change of gene expression compared with control.

Western Blot Analysis

Proteins were prepared from cells, liver, or adipose tissue, resolved by SDS-PAGE, and transferred to nitrocellulose membrane for immunoblotting analysis using specific antibodies, as previously described.[51] Briefly, tissue or cells were homogenized in the lysis buffer (25 mM Tris-Cl [pH 7.4], 50 mM sodium pyrophosphate, 100 mM sodium fluoride, 10 mM EDTA, 1% NP-40, 1 mM phenyl-methyl-sulfonyl fluoride, 10 mM sodium orthovanadate, 10 μg/ml aprotinin, and 10 μg/ml leupeptin). Samples were solubilized for 30 minutes on ice and centrifuged at 12,000 $\times$ g for 15 minutes at 4 °C. Supernatants were collected, and protein

Table 1. Primer Information

Cyclophilin forward	ACTGAATGGCTGGATGGCAAG
Cyclophilin reverse	TGCCCGCAAGTCAAAAGAAAT
Foxo1 forward	AGATGAGTGCCCTGGGCAGC
Foxo1 reverse	GATGGACTCCATGTCACAGT
Tgfb1 forward	ATCCTGTCCAAACTAAGGCTCG
Tgfb1 reverse	ACCTCTTTAGCATAGTAGTCCGC
αSMA forward	ATGAAGCCCAGAGCAAGAGA
αSMA reverse	ATGTCGTCCAGTTGGTGAT
Col1a forward	GCGAGTGCTGTGCTTTCTG
Col1a reverse	GGTCCCTCGACTCCTACATCT
Col3a forward	GTTCTAGAGGATGGCTGTACTAAACACA
Col3a reverse	TTGCCTTGCGTGTTTGATATTC
Timp1 forward	GGCATCCTCTTGTTGCTATCACTG
Timp1 reverse	GTCATCTTGATCTCATAACGCTGG
Mcp1 forward	CAGGTGTCCCAAAGAAGCTGTAG
Mcp1 reverse	GGGTCAGCACAGACCTCTCTCT
Tnfα forward	GAGAAAGTCAACCTCCTCTCTG
Tnfα reverse	GAAGACTCCTCCCAGGTATATG
Il1b forward	TGTTCTTTGAAGTTGACGGACCC
Il1b reverse	TCATCTCGGAGCCTGTAGTGC
MMP2 forward	CAGAGACCTCAGGGTGACAC
MMP2 reverse	GAAGAAGTTGTAGTTGGCCA
MMP9 forward	GCTCCTGGCTCTCCTGGCTT
MMP9 reverse	GTCCCACCTGAGGCCTTTGA
MMP12 forward	TTTCTTCCATATGGCCAAGC
MMP12 reverse	GGTCAAAGACAGCTGCATCA
iNOS forward	CAGCTGGGCTGT ACA AACCTT
iNOS reverse	CATTGGAAGTGA AGCGGTTCG
il-11 forward	AATTCCCAGCTGACGGAGATCACA
il-11 reverse	TCT ACTCGAAGCCTTGTCAGCACA

concentrations were determined using the BCA-protein assay (Thermo Fisher Scientific Inc). Western blot analyses were performed using 100 μg of tissue lysate or 50 ug of cell lysate. Proteins were resolved by 10% denaturing SDS-PAGE and transferred to PVDF membranes. Blots were blocked in BSA-PBST (5% BSA in phosphate-buffered saline [PBS] with 0.1% Tween 20) for 1 hour, and then incubated with primary antibodies (Table 2) in BSA-PBST for overnight. Blots were washed with PBST 3 times (10 minutes each time) and conjugated to an HRP-coupled secondary antibody before final detection of the conjugate by chemiluminescence (Amersham Biosciences). The signal intensity was measured and analyzed by NIH Image J software.

Nuclear and Cytoplasmic Protein Extraction

Nuclear and cytoplasmic proteins were extracted with NE-PER nuclear and cytoplasmic extraction reagent (Thermo Scientific) as previously described.[51] The cytoplasmic and nuclear extracts were all stored at −80 °C until use.

Primary Hepatocytes Isolation

Primary mouse hepatocytes were isolated and cultured as previously described.[40] Briefly, mice were infused with a calcium-free HEPES-phosphate buffer I (Calcium-free HBSS containing 0.5 mM EGTA and 5.5 mM glucose, 1% penicillin-streptomycin [P/S], pH 7.4). After the color of the liver changed to a light brown color, collagenase-containing buffer II (HBSS with 1.5 mM calcium, 0.5 mg/mL type II collagenase, 5.5 mM glucose, 1% P/S, pH 7.4) was perfused into liver for digestion. After the appearance of cracking on the surface of liver, perfusion was stopped, and the liver was excised into ice-cold serum-free Dulbecco's Modified Eagle Medium (DMEM). Cells from digested liver were teased out and suspended in serum-free DMEM, filtered through a 70-μm cell strainer, and centrifuged at 1700 rpm for 2 minutes at 4 °C. The pallet was washed with serum-free DMEM twice, and mixed with Percoll (adjusted to physiological ionic strength with 10× PBS) to a final concentration of 36% and centrifuged at 1800 rpm for 6 minutes at 4 °C. After removing the supernatant, hepatocyte pellet was washed once with serum-free DMEM and resuspended in DMEM supplemented with 10% fetal bovine serum (FBS) and 1% P/S for 3 hours; after cell attachment, hepatocytes were cultured in serum-free DMEM overnight and then subjected to treatment for further analysis.

Histology

The livers of mice were fixed in 10% neutral buffered formalin; they were then processed into paraffin blocks, sectioned at 5 microns, and stained with H&E (Beijing

Table 2. Antibody Information

Anti-Foxo1	*Cell Signaling Technology*	Cat# 2880 (1:1000 dilution); RRID: AB_2106495
Anti-GAPDH	*Cell Signaling Technology*	Cat# 2118s (1:1000 dilution); RRID: AB_561053
Anti-Col1	*Cell Signaling Technology*	Cat#91144 (1:1000 dilution); RRID: AB_2800169
Anti-αSMA	*Abcam*	Cat# M0851 (1:1000 dilution); RRID: AB_2313736
Anti-Phospho-Smad3 Ser423/425	*Cell Signaling Technology*	Cat# 9520 (1:1000 dilution); RRID: AB_2193207
Anti-Smad3	*Cell Signaling Technology*	Cat# 9523 (1:1000 dilution); RRID: AB_2193182
Anti-TGF-β	*Cell Signaling Technology*	Cat# 3711 (1:1000 dilution); RRID: AB_2063354
Anti-rabbit IgG, HRP-linked antibody	*Cell Signaling Technology*	Cat# 7074 (1:5000 dilution); RRID: AB_2099233
TGF-beta1 monoclonal antibody (9016)	ThermoFisher Scientific	Cat# MAB5-23702 (0.5 μg/ml)
Mouse IgG1 isotype control	ThermoFisher Scientific	Cat# 02-6100 (0.5 μg/ml); RRID: AB_2532935

Huayueyang Biotechnology Co), or Sirius red staining (Beijing Leagene Biotech Co Ltd) to visualize morphological features and fibrosis as previously described.[62]

Serum Biochemistry Analysis

The liver function parameters, such as serum ALT and AST, were analyzed using commercial kits (Beijing Ruizheng Shanda Biological Engineering Technology Co Ltd) by the automatic biochemical analyzer (Beijing Prang New Technology Co Ltd). The antioxidant indicators, such as SOD and MDA contents in liver homogenate were determined using commercial kits (Nanjing Jiancheng Bioengineering Institute) to evaluate.

Peripheral Blood Mononuclear Cell Isolation and Flow Analysis

Peripheral blood was collected from submandibular vein (cheek punch) using EDTA-coated Mini Collect tubes (Greiner Bio-One). For each sample, 50 μl of whole blood was analyzed for myeloid cell immunophenotyping. For flow cytometry analysis, cells were prepared as described.[63] Cells were pre-incubated with anti-FcγR II/III antibody (BD Bioscience) for 15 minutes on ice, followed by 30-minute incubation on ice with BV510 anti-mouse CD45 antigen (Biolegend), eFluor450 anti-mouse CD11b antigen (Thermo Fisher Scientific), APC anti-mouse Ly6C antigen (Thermo Fisher Scientific), BV785 anti-mouse Ly6G antigen (Biolegend), APC-eFluor780 anti-mouse CD115 antigen (Thermo Fisher Scientific), PE anti-mouse CX3CR1 antigen (Biolegend), and FITC anti-mouse CCR2 antigen (Biolegend). After the staining with surface markers, red blood cells were lysed with FACS Lysing solution (BD Bioscience), then followed by cell fixation in 2% PFA on ice for 30 minutes. Calibration was performed using antibodies conjugated CompBeads (BD Bioscience). Cells were washed before data acquisition on Aurora spectral flow cytometer (Cytek Biosciences; configuration 4 L 16 V-14B-10YG-8R). Data were analyzed using FlowJo software (Tree Star Inc).

Isolation and Flow Analysis of Non-parenchymal Cells of Liver

Liver NPCs were isolated following the protocol of a liver dissociation kit (Miltenyi Biotec). Collected NPCs (1×10^6 in a volume of 100 μl of PBS) were washed twice with PBS and incubated with live/dead aqua (Invitrogen) followed by anti-FcγR II/III antibody (BD Bioscience) for 10 minutes on ice, and then stained for 30 minutes on ice with a mixture of fluorescently labeled antibodies against surface markers (CD45, Ly6G, F4/80, and CD11b). The cells were fixed with 2% paraformaldehyde and permeabilized for 30 minutes in Perm/Wash buffer (BD Biosciences), followed by staining with a mixture of fluorescently labeled antibodies against intracellular markers (TNFα and IL-1β) for 30 minutes on ice. Cells were washed before data acquisition on Aurora spectral flow cytometer (Cytek Biosciences; configuration 4 L 16 V-14B-10YG-8R). Data were analyzed using FlowJo software (Tree Star Inc).

RNA Sequencing

The liver samples were sent to the Texas A&M Institute for Genome Sciences and Society (TIGSS) molecular genomics laboratory for RNA extraction and RNAseq. RNA samples were quantified using the Qubit fluorometric RNA assay (Thermo Fisher Scientific) for normalization prior to library preparation. RNA libraries were prepared using the Stranded Total RNA Preparation kit (Illumina) following the manufacturer's instructions. RNAseq was performed on the NovaSeq 6000 (Illumina) instrument that generated 150-base-pair, paired-end sequences. The sequencing run produced approximately 6 million reads per sample and resulted in $\sim$200 $\times$ coverage for each sample.

Statistical Analysis

All data in this experiment are expressed as mean $\pm$ standard error of the mean. Prizm software was used to analyze the data. The Student t-test was used for comparison between 2 groups. One-way analysis of variance was used for comparisons among 3 or more groups. $P < .05$ was considered statistically significant. All authors had access to the study data and had reviewed and approved the final manuscript.

Data Availability

All data from this article are available from the corresponding authors upon request.

References

1. Asrani SK, et al. Burden of liver diseases in the world. Journal of Hepatology 2019;70(1):151–171.
2. Aydin MM, Akcali KC. Liver fibrosis. Turk J Gastroenterol 2018;29(1):14–21.
3. Tsuchida T, Friedman SL. Mechanisms of hepatic stellate cell activation. Nat Rev Gastroenterol Hepatol 2017;14(7):397–411.
4. Ramachandran P, et al. Resolving the fibrotic niche of human liver cirrhosis at single-cell level. Nature 2019;575(7783):512–518.
5. Bataller R, Brenner DA. Liver fibrosis. J Clin Invest 2005;115(2):209–218.
6. Iredale JP. Models of liver fibrosis: exploring the dynamic nature of inflammation and repair in a solid organ. J Clin Invest 2007;117(3):539–548.
7. Clouthier DE, Comerford SA, Hammer RE. Hepatic fibrosis, glomerulosclerosis, and a lipodystrophy-like syndrome in PEPCK-TGF-beta1 transgenic mice. J Clin Invest 1997;100(11):2697–2713.
8. Hayashi H, Sakai T. Biological Significance of Local TGF-beta Activation in Liver Diseases. Front Physiol 2012;3:12.
9. Friedman SL. Mechanisms of hepatic fibrogenesis. Gastroenterology 2008;134(6):1655–1669.
10. Ueberham E, et al. Conditional tetracycline-regulated expression of TGF-beta1 in liver of transgenic mice leads to reversible intermediary fibrosis. Hepatology 2003;37(5):1067–1078.

11. Kanzler S, et al. TGF-beta1 in liver fibrosis: an inducible transgenic mouse model to study liver fibrogenesis. Am J Physiol 1999;276(4 Pt 1):G1059–G1068.
12. Weng HL, et al. Profibrogenic transforming growth factor-beta/activin receptor-like kinase 5 signaling via connective tissue growth factor expression in hepatocytes. Hepatology 2007;46(4):1257–1270.
13. Abreu JG, et al. Connective-tissue growth factor (CTGF) modulates cell signalling by BMP and TGF-beta. Nat Cell Biol 2002;4(8):599–604.
14. Caja L, et al. The transforming growth factor-beta (TGF-beta) mediates acquisition of a mesenchymal stem cell-like phenotype in human liver cells. J Cell Physiol 2011; 226(5):1214–1223.
15. Accili D, Arden KC. FoxOs at the crossroads of cellular metabolism, differentiation, and transformation. Cell 2004;117(4):421–426.
16. Barthel A, Schmoll D, Unterman TG. FoxO proteins in insulin action and metabolism. Trends Endocrinol Metab 2005;16(4):183–189.
17. Haeusler RA, Kaestner KH, Accili D. FoxOs Function Synergistically to Promote Glucose Production. J Biol Chem 2010;285(46):35245–35248.
18. Matsumoto M, et al. Impaired regulation of hepatic glucose production in mice lacking the forkhead transcription factor Foxo1 in liver. Cell Metab 2007; 6(3):208–216.
19. Zhang W, et al. FoxO1 regulates multiple metabolic pathways in the liver: effects on gluconeogenic, glycolytic, and lipogenic gene expression. J Biol Chem 2006; 281(15):10105–10117.
20. Yan L, et al. PP2A regulates the pro-apoptotic activity of FOXO1. J Biol Chem 2008;283(12):7411–7420.
21. Alikhani M, Alikhani Z, Graves DT. FOXO1 functions as a master switch that regulates gene expression necessary for tumor necrosis factor-induced fibroblast apoptosis. J Biol Chem 2005;280(13):12096–12102.
22. Barreyro FJ, et al. Transcriptional regulation of Bim by FoxO3A mediates hepatocyte lipoapoptosis. J Biol Chem 2007;282(37):27141–27154.
23. Liu HY, et al. Hepatic autophagy is suppressed in the presence of insulin resistance and hyperinsulinemia: inhibition of FoxO1-dependent expression of key autophagy genes by insulin. J Biol Chem 2009; 284(45):31484–31492.
24. Fan W, et al. FoxO1 regulates Tlr4 inflammatory pathway signalling in macrophages. EMBO J 2010; 29(24):4223–4236.
25. Yan H, et al. Estrogen improves insulin sensitivity and suppresses gluconeogenesis via the transcription factor Foxo1. Diabetes 2019;68(2):291–304.
26. Schmoll D, et al. Regulation of glucose-6-phosphatase gene expression by protein kinase Balpha and the forkhead transcription factor FKHR. Evidence for insulin response unit-dependent and -independent effects of insulin on promoter activity. J Biol Chem 2000; 275(46):36324–36333.
27. Jais A, et al. Heme oxygenase-1 drives metaflammation and insulin resistance in mouse and man. Cell 2014; 158(1):25–40.
28. Michael MD, et al. Loss of insulin signaling in hepatocytes leads to severe insulin resistance and progressive hepatic dysfunction. Mol Cell 2000;6(1):87–97.
29. Guo S, et al. The Irs1 branch of the insulin signaling cascade plays a dominant role in hepatic nutrient homeostasis. Mol Cell Biol 2009;29(18):5070–5083.
30. Dong XC, et al. Inactivation of hepatic Foxo1 by insulin signaling is required for adaptive nutrient homeostasis and endocrine growth regulation. Cell Metab 2008; 8(1):65–76.
31. Pauta M, et al. Akt-mediated foxo1 inhibition is required for liver regeneration. Hepatology 2016;63(5):1660–1674.
32. Xu R, Zhang Z, Wang F-S. Liver fibrosis: mechanisms of immune-mediated liver injury. Cellular & molecular immunology 2012;9(4):296–301.
33. Seki E, Schwabe RF. Hepatic inflammation and fibrosis: functional links and key pathways. Hepatology 2015; 61(3):1066–1079.
34. Yang J, et al. Monocyte and macrophage differentiation: circulation inflammatory monocyte as biomarker for inflammatory diseases. Biomarker research 2014;2(1):1–9.
35. Tacke F, Zimmermann HW. Macrophage heterogeneity in liver injury and fibrosis. Journal of hepatology 2014; 60(5):1090–1096.
36. Dewidar B, et al. TGF-β in hepatic stellate cell activation and liver fibrogenesis—updated 2019. Cells 2019; 8(11):1419.
37. Angelis E, et al. The role of E2F-1 and downstream target genes in mediating ischemia/reperfusion injury in vivo. Journal of molecular and cellular cardiology 2011; 51(6):919–926.
38. Zellmer S, et al. Transcription factors ETF, E2F, and SP-1 are involved in cytokine-independent proliferation of murine hepatocytes. Hepatology 2010;52(6): 2127–2136.
39. Klotz L-O, et al. Redox regulation of FoxO transcription factors. Redox biology 2015;6:51–72.
40. Wu Y, et al. Novel Mechanism of Foxo1 Phosphorylation in Glucagon Signaling in Control of Glucose Homeostasis. Diabetes 2018;67(11):2167–2182.
41. Adachi M, et al. The forkhead transcription factor FoxO1 regulates proliferation and transdifferentiation of hepatic stellate cells. Gastroenterology 2007;132(4):1434–1446.
42. Pan X, et al. FOXO transcription factors protect against the diet-induced fatty liver disease. Scientific reports 2017;7(1):44597.
43. Ding H-r, et al. Protective properties of FOXO1 inhibition in a murine model of non-alcoholic fatty liver disease are associated with attenuation of ER stress and necroptosis. Frontiers in Physiology 2020;11:177.
44. Lee S, et al. Myeloid FoxO1 depletion attenuates hepatic inflammation and prevents nonalcoholic steatohepatitis. The Journal of Clinical Investigation 2022; 132(14).
45. Das SK, et al. Iron-overload injury and cardiomyopathy in acquired and genetic models is attenuated by resveratrol therapy. Scientific reports 2015;5(1):1–15.
46. Alegre F, Pelegrin P, Feldstein AE. Inflammasomes in liver fibrosis. In: Seminars in liver disease. Thieme Medical Publishers, 2017.

47. Canbay A, Friedman S, Gores GJ. Apoptosis: the nexus of liver injury and fibrosis. Hepatology 2004;39(2):273–278.
48. Takehara T, et al. Hepatocyte-specific disruption of Bcl-xL leads to continuous hepatocyte apoptosis and liver fibrotic responses. Gastroenterology 2004;127(4):1189–1197.
49. Guicciardi M, Gores G. Apoptosis: a mechanism of acute and chronic liver injury. Gut 2005;54(7):1024–1033.
50. Chen Y, et al. Transcription factor Foxo1 mediates TGF-β1-induced apoptosis in hepatocytes. The American Journal of Pathology 2023.
51. Pan Q, et al. Reciprocal regulation of hepatic TGF-β1 and Foxo1 controls gluconeogenesis and energy expenditure. Diabetes 2023.
52. Xu Y, et al. A positive feedback loop of TET3 and TGF-β1 promotes liver fibrosis. Cell reports 2020; 30(5):1310–1318.e5.
53. Mazzocca A, et al. Down-regulation of connective tissue growth factor by inhibition of transforming growth factor β blocks the tumor–stroma cross-talk and tumor progression in hepatocellular carcinoma. Hepatology 2010; 51(2):523–534.
54. Mazzocca A, et al. Tumor-secreted lysophostatidic acid accelerates hepatocellular carcinoma progression by promoting differentiation of peritumoral fibroblasts in myofibroblasts. Hepatology 2011;54(3):920–930.
55. Gupta DK, Singh N, Sahu DK. Article Commentary: TGF-β Mediated Crosstalk between Malignant Hepatocyte and Tumor Microenvironment in Hepatocellular Carcinoma. Cancer Growth and Metastasis 2014;7: CGM. S14205.
56. Valenti L, et al. Increased expression and activity of the transcription factor FOXO1 in nonalcoholic steatohepatitis. Diabetes 2008;57(5):1355–1362.
57. Liu Y, et al. Breviscapine ameliorates CCl4-induced liver injury in mice through inhibiting inflammatory apoptotic response and ROS generation. International journal of molecular medicine 2018;42(2):755–768.
58. Qian H, et al. An HNF1α-regulated feedback circuit modulates hepatic fibrogenesis via the crosstalk between hepatocytes and hepatic stellate cells. Cell research 2015;25(8):930–945.
59. Cabrera-Ortega AA, et al. The role of forkhead box 1 (FOXO1) in the immune system: dendritic cells, T cells, B cells, and hematopoietic stem cells. Critical Reviews^{TM} in Immunology 2017;37(1).
60. Zhang K, et al. Phosphorylation of Forkhead Protein FoxO1 at S253 Regulates Glucose Homeostasis in Mice. Endocrinology 2019;160(5):1333–1347.
61. Zhang K, et al. Hepatic suppression of Foxo1 and Foxo3 causes hypoglycemia and hyperlipidemia in mice. Endocrinology 2012;153(2):631–646.
62. Chen Y, et al. Baihe Wuyao decoction ameliorates CCl4-induced chronic liver injury and liver fibrosis in mice through blocking TGF-beta1/Smad2/3 signaling, anti-inflammation and anti-oxidation effects. J Ethnopharmacol 2020;263:113227.
63. Lian Z, et al. Replacing Saturated Fat With Unsaturated Fat in Western Diet Reduces Foamy Monocytes and Atherosclerosis in Male Ldlr(-/-) Mice. Arterioscler Thromb Vasc Biol 2020;40(1):72–85.

Received March 24, 2023. Accepted August 31, 2023.

Correspondence
Address correspondence to: Yajuan Qi, Department of Pharmacology, School of Basic Medical Sciences, North China University of Science and Technology, 21 Bohai Avenue, Tangshan, Hebei, 063210, China. e-mail: yajuanqi@ncst.edu.cn; or Shaodong Guo, Department of Nutrition, College of Agriculture and Life Sciences, Texas A&M University, Cater-Mattil Hall Rm. 135, TAMU2253, College Station, Texas 77843. e-mail: shaodong.guo@ag.tamu.edu.

CRediT Authorship Contributions

Quan Pan, PhD (Conceptualization: Equal; Data curation: Lead; Formal analysis: Lead; Investigation: Lead; Methodology: Equal; Visualization: Lead; Writing – original draft: Lead; Writing – review & editing: Lead)

Mingming Gao (Formal analysis: Supporting; Investigation: Equal; Visualization: Supporting)

DaMi Kim (Formal analysis: Supporting; Investigation: Supporting; Methodology: Supporting; Visualization: Supporting)

Weiqi Ai (Investigation: Supporting)

Wanbao Yang (Investigation: Supporting; Writing – review & editing: Supporting)

Wen Jiang (Writing – review & editing: Supporting)

Wesley Brashear (Formal analysis: Supporting; Software: Lead)

Yujiao Dai (Investigation: Supporting)

Sha Li (Validation: Supporting)

Yuxiang Sun (Writing – review & editing: Supporting)

Yajuan Qi (Conceptualization: Equal; Methodology: Equal; Project administration: Lead; Writing – original draft: Equal; Writing – review & editing: Supporting)

Shaodong Guo (Conceptualization: Lead; Data curation: Lead; Formal analysis: Lead; Funding acquisition: Lead; Methodology: Lead; Project administration: Lead; Resources: Lead; Supervision: Lead; Writing – review & editing: Lead)

Conflicts of interest
The authors disclose no conflicts.

Funding
This work was supported by National Institutes of Health grants (R01DK095118, R01DK120968, and R01DK124588), the American Diabetes Association Career Development Award (1-15-CD-09), faculty start-up funds from Texas A&M University Health Science Center and AgriLife Research, and the United States Department of Agriculture National Institute of Food and Agriculture grant (Hatch 1010958) to Shaodong Guo (PI). This work was funded, in part, by a grant from the National Institute of Environmental Health Sciences (P30 ES029067).